ISBN: 978-3-95450-227-1 ISSN: 2673-5490 doi:10.18429/JACoW-IPAC2022-THPOTK050

CFD STUDIES OF THE CONVECTIVE HEAT TRANSFER COEFFICIENTS AND PRESSURE DROPS IN GEOMETRIES APPLIED TO WATER COOLING CHANNELS OF THE CROTCH ABSORBERS OF ALBA SYNCHROTRON LIGHT SOURCE

S. Grozavu*, G. Raush†,
Terrassa School of Industrial, Aerospace and Audiovisual Engineering (ESEIAAT), Terrassa, Spain
J.J. Casas‡, C. Colldelram§, M. Quispe¶, ALBA-CELLS Synchrotron, Cerdanyola del Vallés, Spain

Abstract

Currently, the storage ring vacuum chambers of ALBA are protected by 156 crotch absorbers made of copper and Glidcop. After more than 10 years of operation as a third-generation light source, the ALBA II project arose, aiming to transform this infrastructure into a fourth-generation synchrotron. This introduces new challenges in terms of the thermal and mechanical design of the future absorbers.

The absorbers' cooling channels consist of a set of 8-mm-diameter holes parallel to each other and drilled in the body of the absorbers. In each hole, there is a 6x1 mm stainless steel concentric inner tube coiled in spiral wires, whose aim is to enhance the heat transfer. The convective heat transfer coefficients used for the original design of the absorbers come from experimental correlations from the literature, and are applied as a global value for the whole system.

In this work, Heat Transfer-Computational Fluid Dynamics (HT-CFD) studies of the convective heat transfer coefficients and pressure gradients in three different cooling channel geometries are carried out, aiming at leading the way of designing the cooling systems toward the CFD simulations rather than applying global experimental values. This information will be useful for the sizing of the new absorbers for the ALBA II project.

INTRODUCTION

Modern synchrotron light sources widely utilize crotch absorbers to protect the vacuum chambers from synchrotron radiation, and their proper refrigeration is essential for their optimal functioning since they are exposed to very high power densities [1]. The impact of the geometry of the refrigeration capacity of their cooling channels has not been properly reported, and there is little information in the specific literature.

The aim of this research is to perform HT-CFD studies of the fluid inside different refrigeration channel geometries, in order to better understand the heat transfer phenomenon and quantify how conservative or optimistic experimental correlations from the literature are.

* grozavustefania@gmail.com
† gustavo.raush@upc.edu
‡ jcasas@cells.es
§ ccolldelram@cells.es
¶ mquispe@cells.es

METHODOLOGY

The methodology followed for the obtainment of the presented results has been designed in order to set a rigorous foundation above which increased difficulty of simulation could be reliable despite the complex geometry of the problem.

Geometry

This methodology consists in three blocks distinguished by the cooling channels' geometry (depicted in Fig. 2):

1. *Stage 1*: Conventional circular section channel. Simulation of the fluid flow inside a 8 mm diameter channel of 500 mm length.
2. *Stage 2*: Concentric channels. Simulation of the fluid flow along concentric channels formed between the 8 mm diameter orifice and a 6x1 mm pipe inserted inside, leaving a 4 mm length free end where the reversing of the flow occurs.
3. *Stage 3*: Concentric channels with spiral wire. The geometry is equivalent to the latter stage, except for the addition of a 0.9 mm diameter spiral wire wrapped around the exterior of the interior pipe.

Meshing

O-grid structured mesh has been employed for the cylindrical portions and along all the wall boundaries inside the fluid, inflation layers had been introduced for a smooth transition of the mesh until reaching a $y^+ \approx 1$ [2], essential for the proper implementation of $k - \omega$ and SST viscous models. For the complex fluid zones, tetrahedrons have been employed. These characteristics can be observed in Fig. 1.

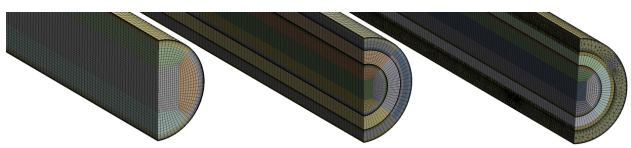

Figure 1: Finest meshes detail of (from left to right): Stage 1 (2.5 M), Stage 2 (5.7 M), and Stage 3 (9.0 M).

Also, a grid convergence study of three levels of mesh refinement has been performed, implementing the 'convergence' Python program provided as a part of the NASA Examining Spatial (Grid) Convergence tutorial [3].

ISBN: 978-3-95450-227-1 ISSN: 2673-5490 doi:10.18429/JACoW-IPAC2022-THPOTK050

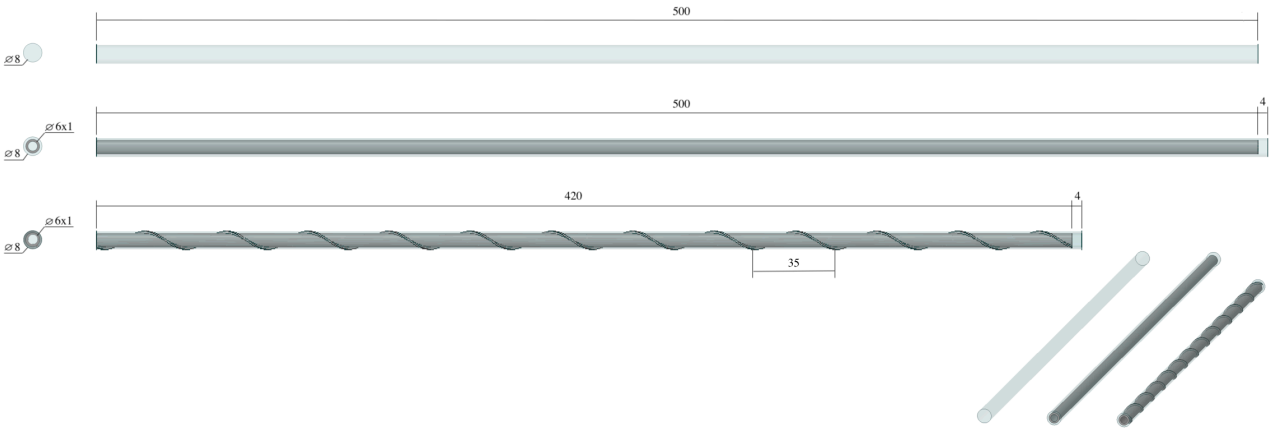

Figure 2: Visual representation and dimensions in mm of the three main cooling channels geometries simulated. From top to bottom: Stage 1 (circular channel), Stage 2 (concentric channels) and Stage 3 (concentric channels with spiral wire).

Boundary Conditions and Solving Methods

For these three stages, simulations with different inlet velocity have been executed, which were selected under ALBA's current criterion of a maximum nominal mean velocity of 3 m/s for cooling channels of thermally critical elements. Inlet temperature of the flow has been set at 23ºC, ALBA's cooling water temperature.

The heat transfer simulations have been modeled as a constant heat flux through the pinhole's copper wall of 80 kW/m^2, resulting in an approximate 1 kW heat power intake. The interior pipe material is defined as steel.

In the first stage, 4 Reynolds Averaged Navier Stocks (RANS) viscous models have been simulated and the results obtained have been compared with the Darcy–Weisbach (D.-W.) equation for pressure drop and the Power-law equation for the developed velocity profile, in order to select the most accurate. These were the $k-\varepsilon$ Realizable, $k-\omega$ Standard, $k-\omega$ Shear-Stress Transport (SST) and Transition SST. The latter model is based on the coupling of the SST $k-\omega$ transport equations with one for the turbulent intermittency and one for the transition onset criteria, which makes it potentially suitable for the modeling of transitional flow [4].

Post-Processing

Since Fluent generated convective heat transfer values are not accurately defined, these will be computed through the following formula [5]:

$$h = \frac{q}{T_w - T_f} \tag{1}$$

where q is the superficial heat flux power, T_w is the wall temperature and T_f, which is the fluid's bulk temperature will be defined as [5]:

$$T_f = \frac{\int \rho c_p u T \, dy}{\dot{m} c_p} \tag{2}$$

In Fluent, the latter expression is virtually equivalent to the Mass Flow Average of the temperature of a transversal area of the fluid.

RESULTS

Stage 1

For three levels of structured mesh of 0.8 M, 1.5 M, and 2.5 M elements, an asymptotic ratio of 0.99876 has been obtained, indicating high accuracy. Transition SST and $k-\omega$ SST models have provided the most similar results to the D.-W. and power-law equations among the four viscous models. For Stage 1, since the Reynolds number finds itself in a range between 18000 and 35000, full turbulence is guaranteed and hence, $k-\omega$ SST model has been employed.

By computing the T_f curve and applying Eq. (1), the local convective coef. has been obtained along the channel's length. This local value resulted constant above $x \approx 0.3\ m$ indicating hydrodynamically and thermally developed flow. For three different velocities (2, 3 and 4 m/s), the coef. in the developed region is depicted in Fig. 3.

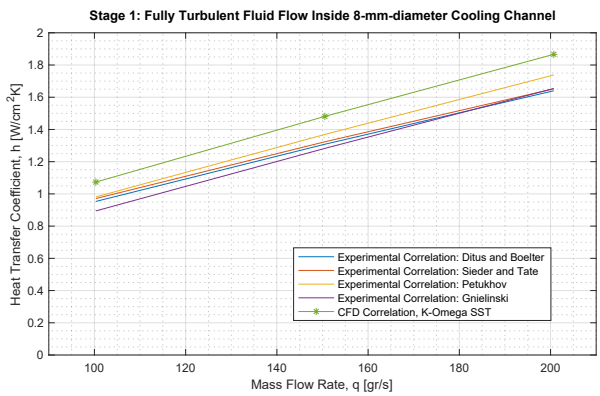

Figure 3: Experimental correlations [6] of the convective coef. contrasted to the CFD values for circular channel flow.

The results from Fig. 3 suggest that the experimental benchmark coefficients, widely employed on the design of cooling channels, contain a relevant conservative element to them. For instance, comparing with Ditus and Boelter's correlation, an increase between 12.6 and 13.8% of the convective heat transfer coefficient has been found.

ISBN: 978-3-95450-227-1 ISSN: 2673-5490 doi:10.18429/JACoW-IPAC2022-THPOTK050

Stage 2

Since the interior to exterior fluid section area ratio is 4:7, the mean flow velocity of the fluid in the exterior annular region is considerably lower than in the interior. Due to this reason, the Reynolds number that defines the exterior flow regime is found in the transition regime, between laminar and turbulent. Thus, applying $k-\omega$ SST model would not be adequate, since the fluid flow would be modeled as fully turbulent even if it is not the case. For this reason, Transition SST model will be employed for comparison purposes since it should adapt to the local flow regime.

Due to lack of references for concentric channels without spiral wires, the results from stage 2 and 3 have been depicted together in Fig. 4 and have been contrasted to the Swiss Light Source (SLS) experimental data [7] for the spiral wires case.

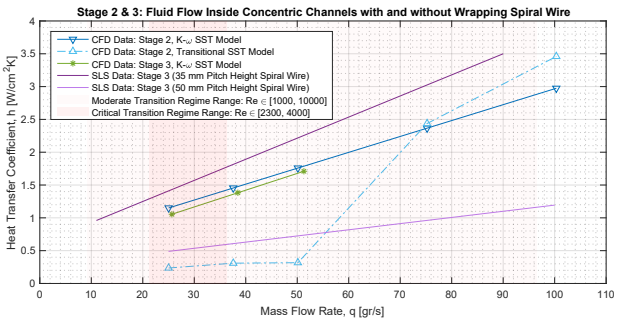

Figure 4: CFD and experimental convective coef. for concentric channels (with and without spiral wires) fluid flow.

The 2nd stage curves from Fig. 4 imply that, in the case of considering a fully turbulent viscous model, the convective coefficient is considerably higher than SLS data for the case of 50-mm-pitch height spiral wires, and modestly lower than the 35-mm-pitch height geometry case. On the other hand, the results of the Transition SST model suggest that for the lower range of velocities, closer or within the critical transition range, the convective coef. decreases dramatically, since the turbulence that has been considered has not been reached. Even so, the results for h are just below the SLS 50-mm-pitch height geometry case for the lower range of fluid velocity, which is highly positive.

Stage 3

For this stage, a shorter pinhole length has been modeled after considering the developed flow distance obtained in the previous stage, thus reducing the computational cost.

Figure 5: Pinhole wall temperature contour and velocities distribution in transversal cross-sections for Stage 3 case.

It is thought that the spiral wire presence enhances turbulence and consecutively, rises the convective coefficient. The interpretation of the CFD results have provided a deeper understanding on the latter. The spiral wire enforces the fluid bulk to flow with a helical tendency. The spiral wiring accelerates the fluid on the "contraction" side (where flow is converged in the spiral motion) but slows it down on the "expansion" side (where flow diverges). Due to this phenomenon, wall temperature follows the spiral distribution (Fig. 5), getting a peak on the low-speed region and a low point on the high-speed region, giving up to a 8 ºC difference in the same cross-section plane. The local h coefficient computed through this T_w follows the same tendency, reversed, obtaining a wide range of values where cooling is improved or worsen. From Fig. 4, the mean h for the 35-mm-pitch height is found to be slightly inferior to the k-ω SST case without spiral wires, which must be studied in more depth.

Lastly, the pressure gradient is reported in Fig. 6 for all three stages. The increase in the pressure drop due to the the spiral wire effect in the exterior fluid region is highlighted.

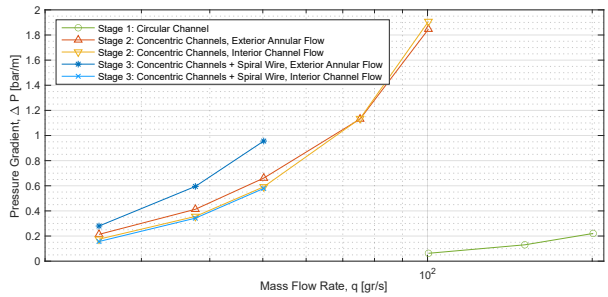

Figure 6: Pressure gradient curves in the developed regions for the three geometries.

CONCLUSION

From this paper, relevant conclusions can be drawn even from the earliest stage, namely the fluid flow along a circular channel. The 14% increase in the convective coefficient of the well founded HT-CFD results over the archaic experimental correlations underlines the oversizing of the systems designed through these guidelines. Many implications derive from this, since in order to attain the same cooling requirements, less water flow rate is truly needed. The most remarkable implications of the latter are: (i) reduction in the pressure drop; (ii) attenuation of the erosion–corrosion effects; (iii) attenuation of the vibration effects, especially concerning for optical components; (iv) reduction in the cost of hydraulic interfaces due to a downsizing in the dimensions; (v) energy saving in the pumping system.

Stages 2 and 3 conclude that further analysis must be carried out since the transition range and the complex geometry create a challenging phenomenon for the CFD analysis. Even so, from stage 3 it can be affirmed that the application of a global convective coefficient in the design of the cooling channels is highly inaccurate and it disregards the temperature peaks that may appear among other effects.

The advance produced by this paper is to take a step further in the HT-CFD analysis of the cooling systems, which is prompt to be the ultimate tool for design purposes in the near future, taking advantage of the great computational power available in today's technology and the major progress achieved in the simulation software's accuracy.

ISBN: 978-3-95450-227-1 ISSN: 2673-5490 doi:10.18429/JACoW-IPAC2022-THPOTK050

REFERENCES

[1] M. Quispe *et al.*, "Development of the Crotch Absorbers for ALBA Storage Ring", in *5th International Conference MEDSI 2008*, Saskatoon, Canada, Jun. 2008, pp. 1-15.

[2] SimScale CAE Forum, https://www.simscale.com/forum/t/what-is-y-yplus/82394

[3] NASA Examining Spatial (Grid) Convergence, https://www.grc.nasa.gov/www/wind/valid/tutorial/spatconv.html

[4] *ANSYS fluent theory guide 15.0*. ANSYS, Canonsburg, PA, Nov. 2013.

[5] A. Neale, D. Derome, B. Blocken and J. Carmeliet, "CFD calculation of convective heat transfer coefficients and validation–Part I: Laminar flow", *Annex 41–Kyoto*, Apr. 2006.

[6] W. Rohsenow *et al.*, "Forced convection, internal flow in ducts", in *Handbook of heat transfer*, vol. 3, NY, USA: McGraw-Hill New York, 1998, pp. 5–27.

[7] G. Heidenreich and L. Schulz (PSI), private communication, 2007.